Article

Cell Reports

Kinase Inhibitor Profiling Reveals Unexpected Opportunities to Inhibit Disease-Associated Mutant Kinases

Graphical Abstract

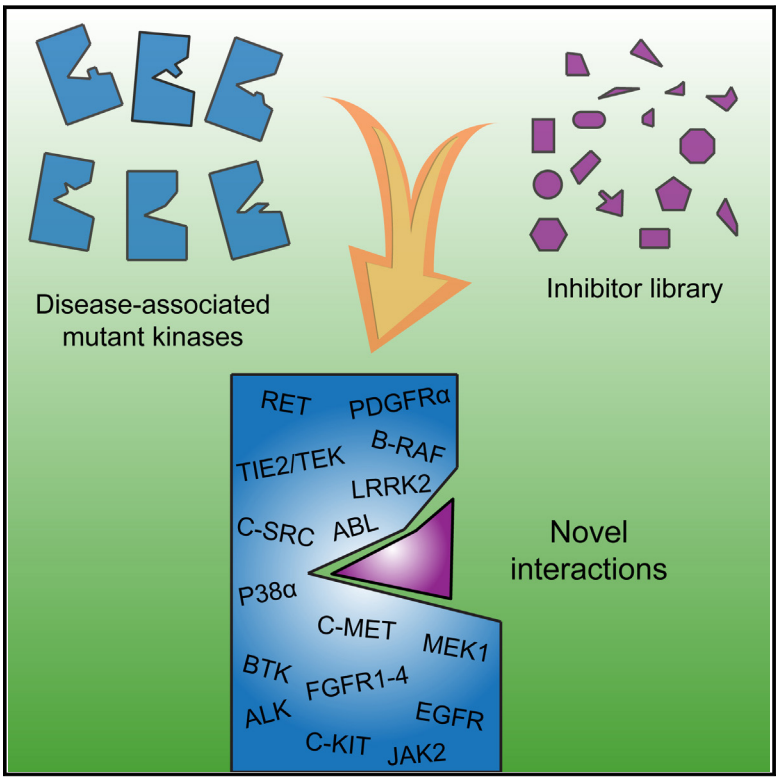

Highlights

- Unbiased screen of 183 small molecule compounds against 76 mutant kinases
- Lead compounds targeting EGFR, PDGFRα, and other mutant kinases
- Opportunities for repurposing FDA-approved kinase inhibitors
- Prediction of chemical modifications to optimize of inhibitors of T674I PDGFRα

Authors

Krisna C. Duong-Ly, Karthik Devarajan, Shuguang Liang, Kurumi Y. Horiuchi, Yuren Wang, Haiching Ma, Jeffrey R. Peterson

Correspondence

jeffrey.peterson@fccc.edu

In Brief

Kinase inhibitors are effective in the clinic, but mutations in kinases can alter inhibitor efficacy. Duong-Ly et al. perform a target-blind screen of 183 small-molecule compounds against 76 mutant kinases to establish a resource for developing agents targeting disease-associated mutant kinases.

Duong-Ly et al., 2016, Cell Reports *14*, 772–781
February 2, 2016
http://dx.doi.org/10.1016/j.celrep.2015.12.080

CellPress

OPEN ACCESS
CellPress

Cell Reports
Article

Kinase Inhibitor Profiling Reveals Unexpected Opportunities to Inhibit Disease-Associated Mutant Kinases

Krisna C. Duong-Ly,[1] Karthik Devarajan,[2] Shuguang Liang,[3] Kurumi Y. Horiuchi,[3] Yuren Wang,[3] Haiching Ma,[3] and Jeffrey R. Peterson[1,*]

[1]Program in Cancer Biology, Fox Chase Cancer Center, 333 Cottman Avenue, Philadelphia, PA 19111, USA
[2]Department of Biostatistics and Bioinformatics, Fox Chase Cancer Center, 333 Cottman Avenue, Philadelphia, PA 19111, USA
[3]Reaction Biology Corporation, 1 Great Valley Parkway, Suite 2, Malvern, PA 19355, USA
*Correspondence: jeffrey.peterson@fccc.edu
http://dx.doi.org/10.1016/j.celrep.2015.12.080

SUMMARY

Small-molecule kinase inhibitors have typically been designed to inhibit wild-type kinases rather than the mutant forms that frequently arise in diseases such as cancer. Mutations can have serious clinical implications by increasing kinase catalytic activity or conferring therapeutic resistance. To identify opportunities to repurpose inhibitors against disease-associated mutant kinases, we conducted a large-scale functional screen of 183 known kinase inhibitors against 76 recombinant mutant kinases. The results revealed lead compounds with activity against clinically important mutant kinases, including ALK, LRRK2, RET, and EGFR, as well as unexpected opportunities for repurposing FDA-approved kinase inhibitors as leads for additional indications. Furthermore, using T674I PDGFRα as an example, we show how single-dose screening data can provide predictive structure-activity data to guide subsequent inhibitor optimization. This study provides a resource for the development of inhibitors against numerous disease-associated mutant kinases and illustrates the potential of unbiased profiling as an approach to compound-centric inhibitor development.

INTRODUCTION

Kinases participate in many signaling pathways, including those involved in cell proliferation, growth, metabolism, apoptosis, and differentiation. Not surprisingly, kinases are mutationally activated in a number of disorders. Small-molecule inhibitor development represents a major focus of drug discovery efforts to treat these disorders. Well over two dozen kinase inhibitors are approved for clinical use by the Food and Drug Administration (FDA) and many others are in clinical development. A major challenge is target promiscuity because most small-molecule kinase inhibitors target the ATP binding site, a highly conserved region in kinases. Therefore, compounds designed to target this site often inhibit other kinases as well (Zhang et al., 2009). Indeed, several recent large-scale screens have revealed numerous off-target effects for both commonly used research tool compounds and clinical kinase inhibitors (Anastassiadis et al., 2011; Davis et al., 2011; Fabian et al., 2005; Gao et al., 2013; Karaman et al., 2008). In some cases, these studies have identified unexpected kinase targets inhibited more potently by a compound than that compound's intended target. Therefore, broad profiling of compounds against kinase libraries can be used for repurposing existing agents based on unexpected activity against unrelated kinases.

One particularly exciting application of broad profiling is the identification of potent and selective inhibitors of mutant kinases. Disease-associated kinase domain mutations can increase kinase activity. Well characterized examples of activating, disease-associated kinase mutations are deletions in exon 19 of the epidermal growth factor receptor (EGFR) present in non-small-cell lung cancer (NSCLC). Normally, ligand binding promotes EGFR dimerization and auto-activation. Deletions in exon 19 promote EGFR dimerization and auto-activation in the absence of ligand, leading to constitutive kinase activity (Ladanyi and Pao, 2008).

Although exon 19-deleted mutants of EGFR are generally sensitive to erlotinib and gefitinib, therapeutic use of kinase inhibitors can select for mutations that render these kinases resistant to these therapies. A common hotspot for resistance mutations in many kinases is the gatekeeper residue located within the ATP-binding pocket. Gatekeeper mutations can enhance ATP binding affinity or sterically restrict inhibitor binding, thereby reducing inhibitor potency. The T790M gatekeeper residue mutation in EGFR, for example, increases ATP affinity and confers erlotinib and gefitinib resistance (Pao et al., 2005; Yun et al., 2008). Another classic example is the T315I mutation in the BCR-ABL kinase, which confers imatinib resistance (Gorre et al., 2001). In some instances, resistance mutations also enhance kinase catalytic activity (Azam et al., 2008).

In recent years, improved sequencing technologies have facilitated the identification of activating and resistance mutations in

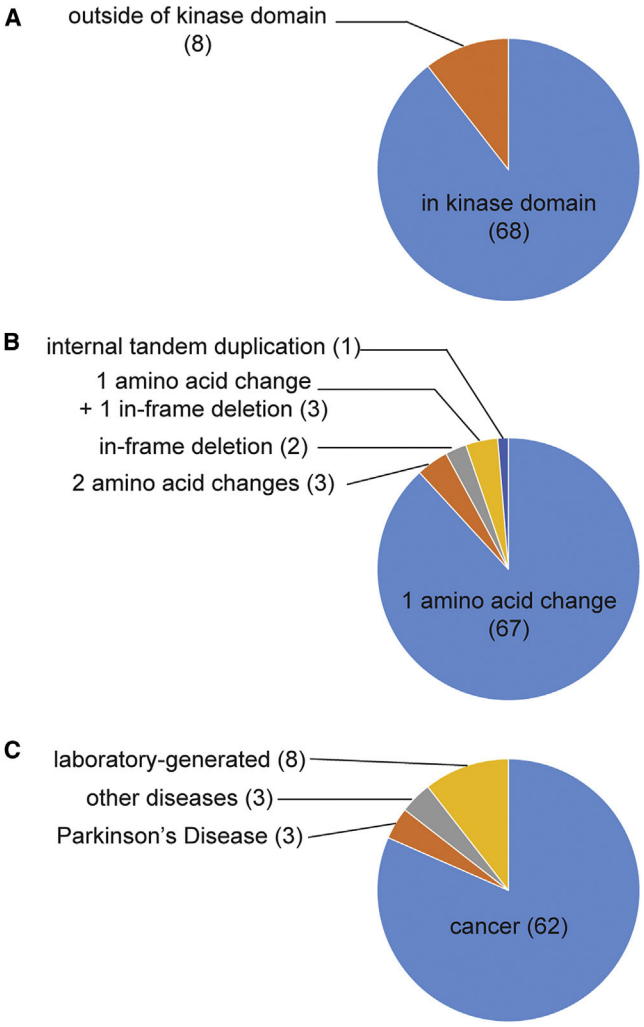

Figure 1. The Mutated Kinases Represent a Diverse Set of Kinase Variants

(A) Distribution of kinase variants containing alterations in the kinase domain versus outside of the kinase domain.

(B) Distribution by mutation type.

(C) Disease association of kinase variants. "Laboratory-generated" reflects mutations that have not been associated with any physiological disorders.

A complete list of mutated kinases is available in Table S1.

kinases. We have previously performed a target-blind screen of 178 compounds against a panel of 300 wild-type protein kinases to examine kinase inhibitor selectivity (Anastassiadis et al., 2011). Although this dataset provided a wealth of information about clinical kinase inhibitors, compounds in clinical development, and research tool compounds, it did not provide insights into inhibition of clinically relevant mutant kinases. Here we screened an overlapping collection of 183 small-molecule compounds against a panel of 76 mutated kinases derived from 21 cognate wild-type kinases. The resulting dataset comprises over 13,000 mutant kinase-compound pairs, almost an order of magnitude larger than those of prior studies (Davis et al., 2011; Uitdehaag et al., 2014). These mutated kinases include many drug-resistant kinases and activating disease-associated mutant kinases. The data not only faithfully reproduced known kinase/inhibitor interactions but also revealed several targets and opportunities for repurposing FDA-approved kinase inhibitors against disease-relevant targets. We found an inhibitor of the highly resistant T790M EGFR mutant that, although related structurally and mechanistically, is more selective than afatinib, an FDA-approved agent. We also describe a series of clinical compounds that inhibit imatinib-resistant T674I platelet-derived growth factor receptor α (PDGFRα) and demonstrate how the data can be used not only to identify lead inhibitor scaffolds against kinases of clinical interest but also to generate predictive structure-activity hypotheses for lead compounds that can guide their subsequent optimization. We further anticipate that this dataset will serve as a useful resource for the development of compounds active against other disease-associated kinase variants.

RESULTS

Screening of a Broad Panel of Mutated Kinases

A total of 183 small-molecule compounds were screened against 76 mutant kinases (Experimental Procedures; Table S1) using the HotSpot radiometric filter-binding kinase assay (Anastassiadis et al., 2011). This functional assay directly measures kinase-catalyzed transfer of a radiolabeled phosphate from ATP to a relevant protein or peptide substrate. The compounds screened included 12 that are FDA-approved. Other compounds included those in clinical development and research tool compounds. All compounds were screened in duplicate at 500 nM in the presence of 10 μM ATP to reveal weak off-target activities and for consistency with our previous analysis with wild-type kinases (Anastassiadis et al., 2011).

The vast majority of the mutated kinases contain alterations in the kinase domain (Figure 1A). Most variants are single amino acid changes, but there are also variants with one in-frame deletion each (d746–750 EGFR and d752–759 EGFR), three variants containing two amino acid changes (L858R/T790M EGFR, V559D/V654A C-KIT, and V559D/T670I C-KIT), an internal tandem duplication (FLT3 ITD), and three variants containing both an in-frame deletion and an amino acid change (d746–750/T790M EGFR, d747–749/A750P EGFR, and d747–752/P753S EGFR; Figure 1B). Over 80% of the kinases are cancer-associated variants documented by the COSMIC database (Forbes et al., 2011) or elsewhere (Figure 1C). The remaining kinases represent variants present in other diseases or laboratory-generated mutations. One-third of the kinase constructs represent acquired resistance mutations found in patients who relapse following treatment. The kinases arise from a total of 21 corresponding wild-type kinases, comprising 16 tyrosine and five serine/threonine kinases. The over-representation of tyrosine kinases compared with their representation in the human kinome reflects the historical focus on this kinase subfamily in drug discovery.

The data comprise 13,875 mutant kinase/compound pairs. For each kinase/compound interaction, we calculated the percent remaining kinase activity relative to a control reaction in the presence of vehicle (dimethyl sulfoxide). Each measurement was performed in duplicate, and 33 discrepant data pairs (0.2% of the dataset) were identified and eliminated as described

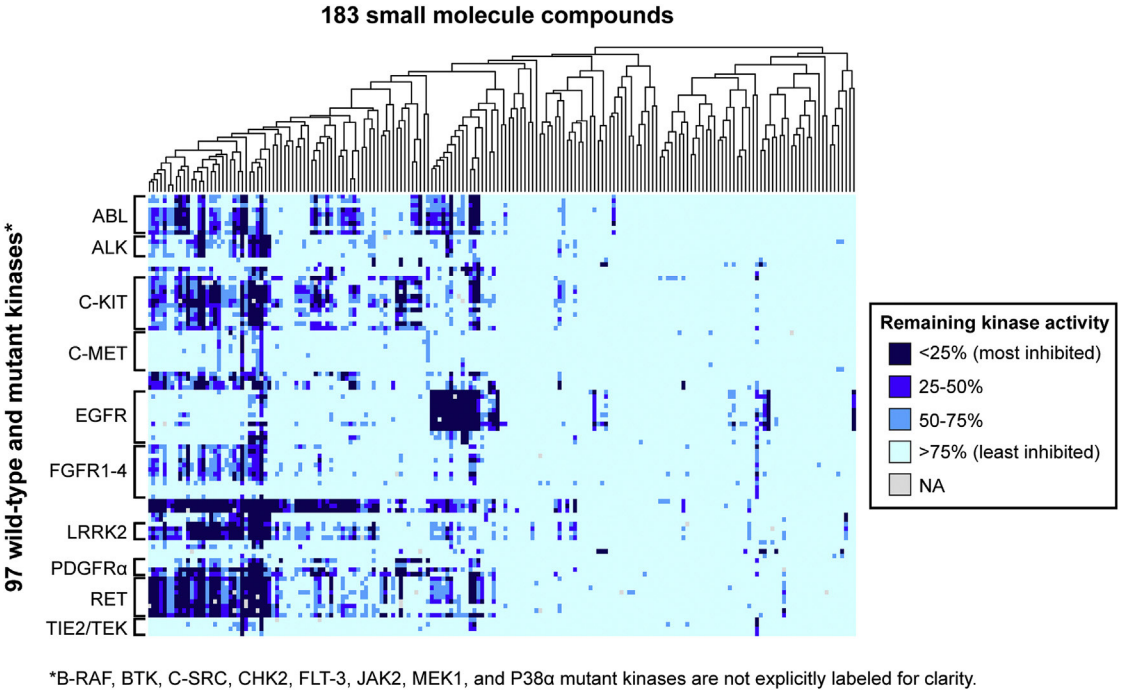

Figure 2. Large-Scale Screen of Kinase/Compound Pairs

Shown is a heatmap representing the distribution of remaining kinase activities for kinase/compound pairs in this study as well as data for their wild-type cognates, as reported previously (Anastassiadis et al., 2011). The 183 compounds in the screen were subjected to hierarchical clustering, as shown by the dendrogram at the top. The 76 mutant kinases are grouped according to cognate wild-type kinase. Only kinase families with three or more members are labeled for clarity. A fully labeled version of this figure is provided in Figure S1; and the complete dataset is available in Table S2 and can be searched at the Kinase Inhibitor Resource (kir.fccc.edu).

previously (Anastassiadis et al., 2011). Importantly, we have shown previously that single-dose screening from this platform is recapitulated reliably in follow-up dose-response experiments (Anastassiadis et al., 2011), and we confirm this reproducibility again below. The data are presented as a heatmap in Figure 2 (a higher-resolution figure with labels is available as Figure S1, and the complete dataset is available in Table S2 and can be queried at the Kinase Inhibitor Resource [kir.fccc.edu]) and include data reported previously for the corresponding wild-type forms for comparison (Anastassiadis et al., 2011). The compounds exhibited a wide range of selectivity. 39% of compounds did not inhibit any mutant kinase by >50%, whereas 7.1% of compounds inhibited half or more of the mutant kinases by >50%. Only 3.8% of compounds inhibited a single mutant kinase target by >50%.

For the most part, mutant kinases are inhibited by compounds that also inhibit their cognate wild-type kinases (Anastassiadis et al., 2011). However, resistance mutations and mutations that enhance kinase sensitivity to particular compounds are also present. Also, a number of unexpected compound/kinase interactions were revealed from the single-dose screening data that were subsequently verified in dose-response experiments and warrant further investigation. For example, we found that the tool compounds Flt-3 inhibitor and Jak3 inhibitor II also inhibit Parkinson's disease-associated LRRK2 mutants (Figures S2A and S2B; Table S3). Also, we identified bosutinib isomer as an inhibitor of crizotinib-resistant L1196M ALK (Figure S2C; Table S3). Additionally, we showed that tozasertib, a serine/threonine kinase inhibitor, can inhibit mutants of the RET tyrosine kinase (Figure S2D; Table S3). Below we discuss in greater detail just two examples of previously undescribed compound-kinase interactions, including a highly selective inhibitor of the T790M EGFR mutation that is structurally similar to afatinib but with fewer non-EGFR family targets and several clinical kinase inhibitors that inhibit imatinib-resistant T674I PDGFRα.

Comparison with Previous Studies

A small proportion of the analyzed mutant kinase/compound pairs overlaps with previous large-scale screens (Tables S4 and S5). 1.9% of the mutant kinase/compound pairs overlapped with a previous study that utilized either ELISA or mobility shift assays to measure inhibition of kinase activity by 1 μM compound (Uitdehaag et al., 2014). For kinase/compound pairs that overlapped with our study (Table S4), there was general agreement, with the majority of overlapping pairs (66%) displaying either no inhibition or nearly complete inhibition of kinase activity in both studies (boxed regions in Figure 3A). Kinase/compound pairs with intermediate levels of inhibition (values outside of the boxed regions in Figure 3A) showed greater discrepancies, likely because of the sensitivity of the assay to small differences in compound concentration near the IC_{50} value or differences in the methods or protein constructs employed. Overall, 79% of the

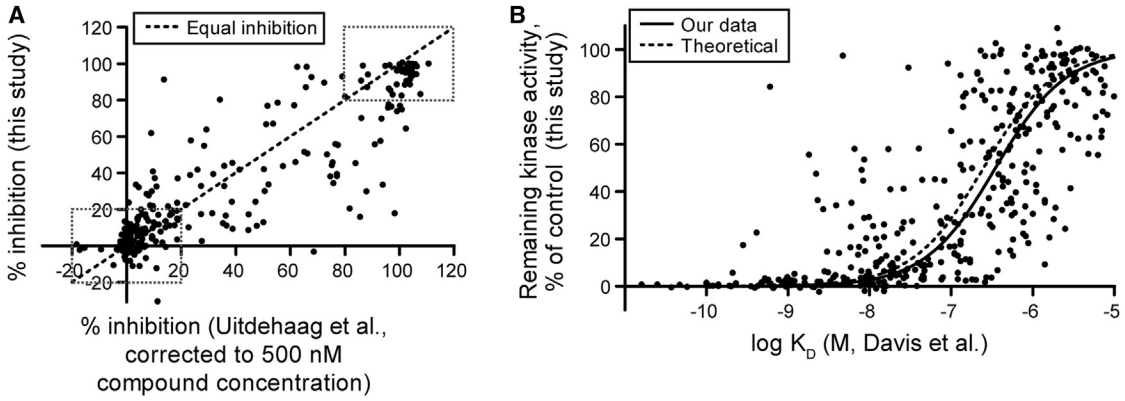

Figure 3. Comparison of Overlapping Data between This Screen and Previous Studies

(A) Percent inhibition from the Uitdehaag et al. (2014) study was extrapolated to 500 nM, as described previously (Anastassiadis et al., 2011), and was plotted against percent inhibition in this study. Dashed boxes indicate compound/kinase interactions that fall within 20% of complete inhibition or 20% of no inhibition. The dashed line denotes the line of identity between the two studies. The complete list of overlapping pairs between these studies is given in Table S4. WT, wild-type. (B) Remaining kinase activity from this screen was plotted against binding affinities from Davis et al. (2011). The solid line represents a fit to a standard sigmoidal dose-response curve. The dashed line represents a theoretical curve for remaining kinase activity derived as described in Anastassiadis et al. (2011). The complete list of overlapping pairs between these studies is given in Table S5.

overlapping pairs exhibit either no inhibition, nearly complete inhibition, or show remaining kinase activity values within 20% of each other between the studies when the data from Uitdehaag et al. (2014) are extrapolated to 500 nM compound concentration according to the Cheng-Prusoff equation (Figure 3A).

A fraction (2.7%) of the mutant kinase/compound pairs in our study also overlap with another large-scale kinase/compound interaction study (Davis et al., 2011) that utilized a competitive binding assay rather than an enzymatic assay. For the overlapping pairs between the two screens (Table S5), the percent remaining kinase activity measured in the functional assay and the affinities measured in the binding assay were compared using the Cheng-Prusoff equation (Figure 3B). The results of both studies are highly congruent, with compounds exhibiting high-affinity binding also generally showing potent inhibition in the functional assay. In some cases, however, the results of the two assays differed significantly (e.g., C-KIT V559D/V654A-masitinib and C-KIT A829P-staurosporine). In these cases, the binding assay reported a K_D of <5 nM, but only moderate kinase inhibition was observed at 500 nM. Such discrepancies could reflect differences in the kinase constructs used in the two studies or, more interestingly, differences in kinase activation state, perhaps resulting from the presence (this study) or absence (Davis et al., 2011) of ATP in the screen. These discrepancies warrant further investigation. However, the overall congruence of these studies, which utilize distinct assays to monitor compound-kinase interactions, supports the reliability of the data.

Inhibition of a Resistant Target, T790M EGFR

Several EGFR mutations found in NSCLC lead to increased kinase activity and, in some cases, ligand-independent activation (Pines et al., 2010). Our mutant kinase panel contains 11 variant forms of EGFR, eight of which are clinically relevant activated forms, including exon 19 deletion mutations (d746–750, d747–749/A750P, d747–752/P753S, and d752–759) and activating point mutations (G719C, G719S, L858R, and L861Q). Together, these mutations account for >90% of all activating EGFR mutants reported in NSCLC (Ladanyi and Pao, 2008). Consistent with previous studies, we found that these EGFR mutants were sensitive to the FDA-approved EGFR inhibitors erlotinib and gefitinib (Figure 4A).

Although these activated EGFR variants are generally sensitive to erlotinib and gefitinib, acquired resistance occurs in 50% of patients treated with these agents (Balak et al., 2006; Carey et al., 2006; Paez et al., 2004). About half of the patients with acquired resistance harbor the T790M mutation (Kosaka et al., 2006). In addition, 5% of untreated NSCLC patients also express T790M EGFR and have primary resistance to erlotinib and gefitinib (Bell et al., 2005). Our mutant kinase panel includes three erlotinib/gefinitib-resistant EGFR forms, all of which contain the T790M mutation (T790M, T790M/L858R, and d746–750/T790M). T790M EGFR mutants were among the most inhibitor-resistant kinases in our screen. Although 22% of the screened compounds inhibited at least one of the EGFR mutants by at least 50%, only 7% of the screened compounds inhibited at least one of the T790M EGFR mutants by the same amount (Figures 4A and 4B; Table S2). One of these, afatinib, is an FDA-approved EGFR inhibitor for NSCLC with known activity against T790M EGFR (Katakami et al., 2013; Li et al., 2008). As expected, afatinib potently inhibited T790M and other EGFR mutants in the panel (Figure 4A).

One additional compound showed similarly potent and selective inhibitory activity against the T790M mutant: EGFR/ErbB2/ErbB4 inhibitor (CAS no. 881001-19-0; Figures 4B and 4C; Table S2; Figure S3). This compound was developed to target the ErbB family (Klutchko et al., 2006), but its potency against EGFR variants harboring the T790M mutation has not been reported previously. Surprisingly, comparing its chemical structure to that of afatinib revealed striking similarities (Figure 4C). Both compounds are inhibitors that covalently bind to cysteine 797 in EGFR and were developed through two independent drug

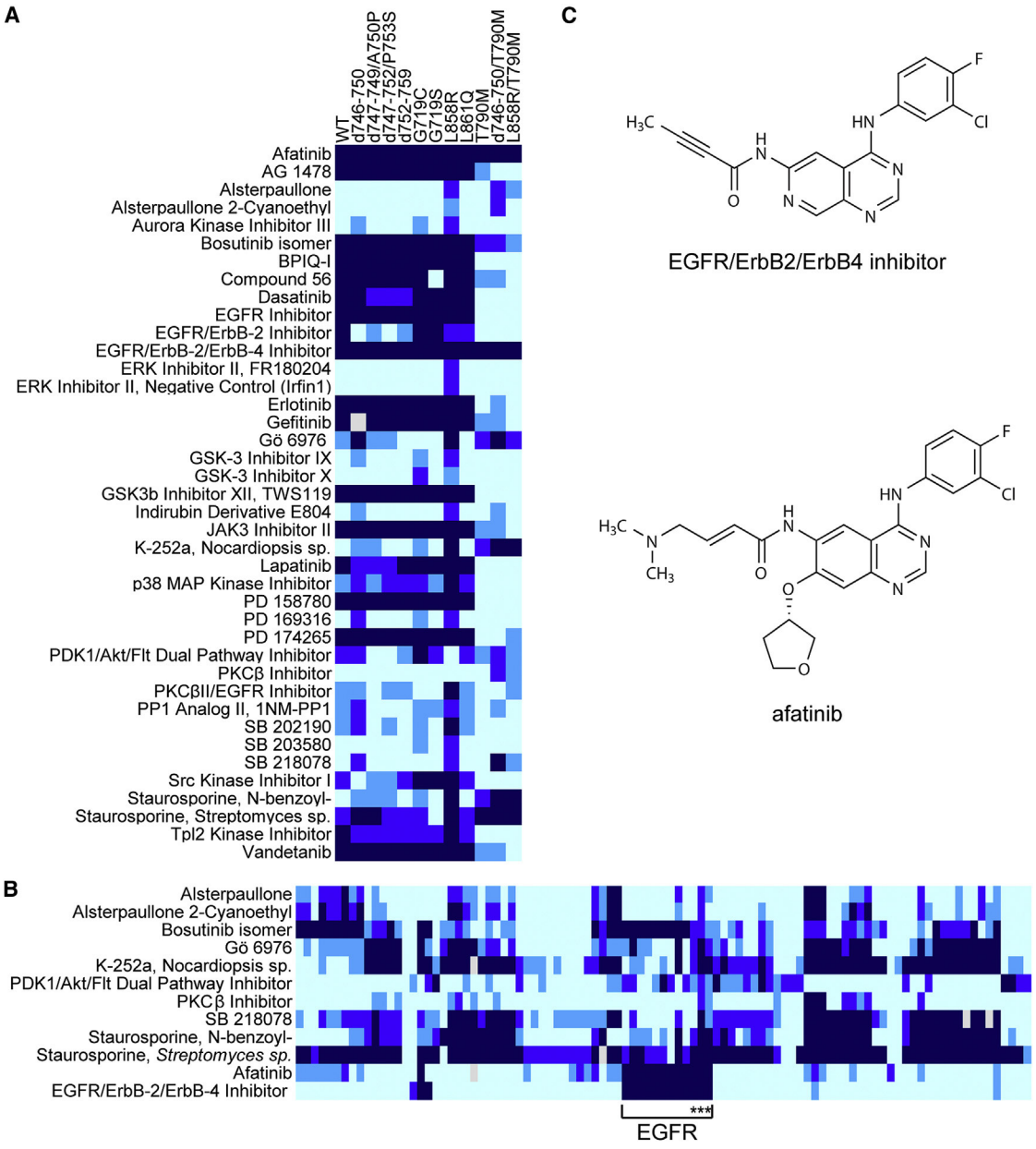

Figure 4. The EGFR/ErbB2/ErbB4 Inhibitor and Afatinib Inhibit T790M EGFR

(A) Heatmap representing compounds that inhibit any EGFR mutants with less than 50% remaining kinase activity. The coloring is as shown in Figure 2.

(B) Heatmap representing compounds that inhibit one or more of the T790M EGFR mutants with less than 50% remaining kinase activity. The EGFR family is indicated with the bracket, and the EGFR variants containing T790M are indicated with asterisks. An explicitly labeled heatmap is provided in Figure S3.

(C) Chemical structures of the EGFR/ErbB2/ErbB4 inhibitor and afatinib.

discovery efforts (Eskens et al., 2008; Klutchko et al., 2006). Although both compounds inhibit all T790M EGFR kinases with low nanomolar IC_{50} values (Figure S4), the EGFR/ErbB2/ErbB4 inhibitor exhibited greater selectivity than afatinib based on its Gini coefficient, a metric of kinase inhibitor selectivity (Graczyk, 2007). The Gini coefficient for the EGFR/ErbB2/ErbB4 inhibitor is 0.791 versus 0.712 for afatinib when screened against a panel of 300 wild-type kinases (Table S6). Of the ten kinases inhibited by the EGFR/ErbB2/ErbB4 inhibitor by more than 50%, eight have a Cys residue in the position analogous to EGFR Cys797 (BLK, BMX/ETK, BTK, EGFR, ERBB2, ERBB4, JAK3, and TXK) whereas two (CLK3 and RIPK2) do not. In contrast, of the 19 kinases inhibited by afatinib by more than 50%, only six (BLK, BTK, EGFR, ERBB2, ERBB4, and TXK) have a Cys residue at this position whereas 13 (C-MER, C-SRC, EPHA6, EPHB4, FGR, HCK, IRAK1, LCK, LYN, MNK1, MNK2, P38α/MAPK14, and YES/YES1) do not. These data imply that afatinib inhibits these kinases without forming a covalent adduct at the position

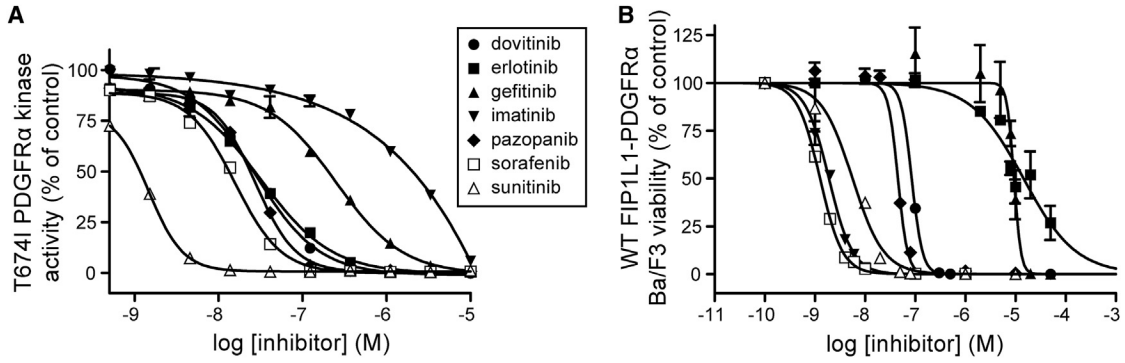

D

cell line IC50, nM (95% CI)

	WT	T674I
dovitinib	85.6 (78.1-93.8)	436 (404-472)
erlotinib	14500 (10300-20400)	1640 (1260-2130)
gefitinib	9340 (8480-10300)	6200 (5440-7060)
imatinib	1.91 (1.77-2.06)	13600 (11800-15700)
pazopanib	45.2 (42.0-48.7)	3170 (2920-3440)
sorafenib	1.27 (1.22-1.32)	144 (116-179)
sunitinib	5.63 (4.13-7.68)	45.2 (40.9-49.9)

Figure 5. Several Clinical Kinase Inhibitors Target T674I PDGFRα

(A) Dose-response curves based on in vitro kinase assays against recombinant T674I PDGFRα. IC_{50} values are given in Table S3. Error bars represent SEM.

(B) Cell viability measurements of Ba/F3 cells expressing WT FIP1L1-PDGFRα in the presence of the same compounds tested in (A). Error bars represent SEM.

(C) The same as (B) but for Ba/F3 cells expressing T674I FIP1L1-PDGFRα.

(D) IC_{50} values for the cell viability measurements in (B) and (C).

analogous to EGFR Cys797. Such a mechanism could explain the lower selectivity of afatinib compared with the EGFR/ErbB2/ErbB4 inhibitor. The potency and selectivity of the EGFR/ErbB2/ErbB4 inhibitor suggests that it warrants further study.

Repurposing Clinical Kinase Inhibitors to Target T674I PDGFRα

Repurposing clinical agents for use against additional kinases beyond the intended target is attractive because the safety of these agents has already been established. We were therefore particularly interested in targets for compounds in our panel that are either FDA-approved or in clinical development. One target of several clinical agents was the T674I mutant of PDGFRα. This mutation occurs clinically in the context of a fusion protein resulting from a chromosomal translocation that joins the first 233 amino acids of the Fip1-like 1 protein (FIP1L1) and the last 523 amino acids, including the kinase domain, of PDGFRα (Cools et al., 2003). Kinase activity of the resultant FIP1L1-PDGFRα protein is associated with hypereosinophilic syndrome (HES) (Cools et al., 2003), a myeloproliferative disorder of eosinophils that can progress to chronic eosinophilic leukemia (CEL). Patients expressing wild-type FIP1L1-PDGFRα respond to imatinib, but acquisition of the T674I mutation renders the cells imatinib-resistant (Cools et al., 2003). Several kinase inhibitors, including sorafenib and nilotinib, have shown only limited clinical efficacy in imatinib-resistant HES and CEL (von Bubnoff et al., 2006; Lierman et al., 2006, 2009; Metzgeroth et al., 2012). Ponatinib, a multi-targeted tyrosine kinase inhibitor, has shown promising activity in cell lines expressing T674I FIP1L1-PDGFRα but has not yet been evaluated in patients with this mutation (Sadovnik et al., 2014). Therefore, there is a need for second-line therapies for HES/CEL associated with T674I FIP1L1-PDGFRα.

Consistent with previous studies (Cools et al., 2003), our screening data indicated that T674I PDGFRα is substantially resistant to imatinib (IC_{50} = 1.48 μM; Figure 5A; Table S3). Our screen also revealed several additional clinical agents, including dovitinib, erlotinib, pazopanib, sunitinib, and sorafenib, that inhibited T674I PDGFRα by >90% at the 500 nM screening concentration (Table S2). Only sorafenib and sunitinib have been noted previously to be active against T674I FIP1L1-PDGFRα (Lierman et al., 2006; Sadovnik et al., 2014). Dose-response experiments were conducted against recombinant T674I PDGFRα with each of these compounds as well as with gefitinib, which

shares structural similarity with erlotinib. Of all of these agents, sunitinib was the most potent (IC_{50} = 1.17 nM; Figure 5A; Table S3), although all, with the exception of gefitinib, exhibited low nanomolar IC_{50} values consistent with the primary screening data.

We then tested whether or not these compounds inhibit the proliferation of Ba/F3 cell lines that are dependent on either wild-type FIP1L1-PDGFRα or T674I FIP1L1-PDGFRα for growth (Cools et al., 2003; Figures 5B–5D). As expected (Cools et al., 2003), imatinib was much more effective at inhibiting the growth of wild-type FIP1L1-PDGFRα Ba/F3 cells (IC_{50} = 1.91 nM) than T674I FIP1L1-PDGFRα cells (IC_{50} = 13.6 μM). Sunitinib potently inhibited T674I FIP1L1-PDGFRα cell growth (IC_{50} = 45.2 nM), consistent with the in vitro data and a recent report (Sadovnik et al., 2014), and two additional FDA-approved agents, sorafenib and pazopanib, showed significant anti-proliferative activity (144 nM and 3.17 μM, respectively). These results argue for immediate consideration of these agents as potential second-line therapies for imatinib-resistant CEL. In addition, dovitinib also potently inhibited growth of the mutant-expressing cells (IC_{50} = 436 nM), although this compound has not yet received FDA approval. Although most tested agents showed more potent inhibition of wild-type FIP1L1-PDGFRα-expressing cells than the T674I mutant (Figures 5B–5D), gefitinib showed comparable anti-proliferative activity against both cell lines (9.34 μM versus 6.20 μM). More strikingly, erlotinib inhibited T674I mutant cells more than 8-fold more potently than cells expressing the wild-type fusion (1.64 μM versus 14.5 μM). This unexpected selective activity against T674I demonstrates a potential therapeutic window for activity against the cancer-associated mutation compared with the wild-type form that could be exploited further through additional medicinal chemistry as discussed below.

Prediction of Chemical Modifications that Affect the Potency of 4-Anilinoquinazolines against T674I PDGFRα

Primary screening hits must generally be optimized to increase their potency as lead compounds. However, structurally related compounds in the screening library can often provide important clues regarding the underlying structure-activity relationship and guide medicinal chemistry efforts. 13 of the 183 compounds screened in this study contain the 4-anilinoquinazoline core found in erlotinib (Table S7). Interestingly, these compounds exhibited a wide range of inhibitory potency against T674I PDGFRα (Table S7). Because structure-guided design of inhibitors against PDGFRα is not possible because of the lack of high-resolution structural data for this kinase, we examined whether our screening data could be used to predict chemical modifications to 4-anilinoquinazoline that could guide the development of more potent anilinoquinazolines with activity against T674I PDGFRα.

All of the 4-anilinoquinazoline compounds included in the screen were substituted at either the meta and/or para positions of the aniline ring. Only vandetanib contained a substituent at the ortho position. To determine whether substitutions at the meta or at the para position were generally associated with more potent T674I inhibition, we compared the single-dose activity of all 13 4-anilinoquinazoline compounds (Figure 6A). Although these compounds differed at other positions as well, we observed a modestly greater average inhibitory activity among compounds containing substituents at the meta position. In addition, larger substituents at the para position were associated with lower potency (Figure 6B). Halogens (either Br or Cl) were often present at the meta position of the aniline ring, and compounds with Br at this position had, on average, a slightly greater potency compared with those containing Cl, suggesting that either electronegativity and/or atomic size had an effect on compound potency toward T674I PDGFRα (Figure 6C). We next considered whether these aggregate trends revealed by the single-dose profiling data reflected true underlying structure-activity relationships.

To rigorously test our structure-activity hypotheses in the context of otherwise identical 4-anilinoquinazoline compounds, we obtained a variety of derivatives of 6,7-dimethoxy-4-anilinoquinazoline (Figure 6D), confirmed their identity and purity by liquid chromatography-mass spectrometry (LC-MS), and measured inhibitory activity at multiple doses against T674I PDGFRα. To test whether meta substitutions are generally preferred over para substitutions, we compared the potency of WHI-P180 (compound 1) and Janex 1 (compound 2). Confirming our prediction, the meta-substituted compound 1 was indeed more potent by a factor of 2-fold (Figure 6E).

We next tested whether a series of compounds with increasingly larger para substituents (Janex 1 [compound 2] < Src kinase inhibitor I [compound 3] < EGFR/ErbB2 inhibitor [compound 4]) showed decreased inhibitory potency. Although compound 3 was several fold more potent than compound 4, as predicted, compound 2 was approximately 2-fold less potent than compound 3 (Figure 6F), possibly because of confounding effects of the hydrogen-bonding capacity of compound 2. These observations highlight the complexity of validating structure-activity hypotheses from a limited numbers of compounds, but, collectively, our data suggest a general trend that larger substituents at the para position of the aniline ring decrease compound potency.

Last, we examined whether less electronegative/larger halogens have enhanced potency compared with more electronegative/smaller halogen atoms at the meta position of the aniline ring of the 6,7-dimethoxy-4-anilinoquinazoline pharmacophore. Although the Br-substituted PD153035 (compound 6) and the $Cl^{\square}$ substituted AG-1478 (compound 5) had similar IC_{50} values for inhibition of T674I PDGFRα kinase activity, these compounds were approximately 1.5-fold more potent than the more electronegative, smaller fluoride-substituted compound 7, in agreement with our prediction (Figure 6G). Collectively, these comparisons demonstrate that the screening data presented in this study can be used to infer chemical modifications that enhance inhibitor potency in the absence of any structural data for a kinase.

DISCUSSION

Mutations in kinases can result in deregulated kinase activity that can promote diseases such as cancer. Although pharmacological inhibition with small molecules can lead to tumor regression, many kinase targets develop resistance through secondary mutations. Another challenge in the development of kinase

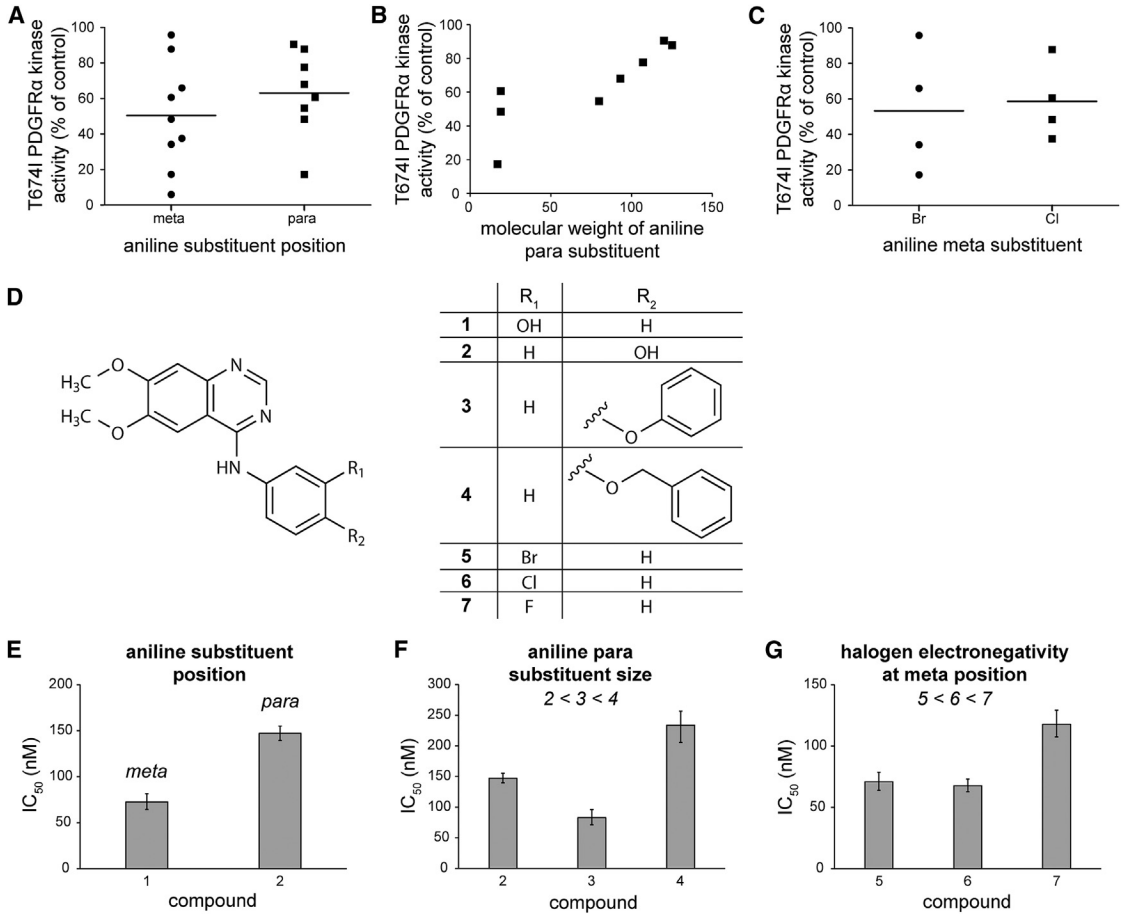

Figure 6. Chemical Modifications Affecting the Potency of 4-Anilinoquinazoline Compounds toward T674I PDGFRα

(A) Remaining kinase activity of T674I PDGFRα in the presence of 4-anilinoquinazolines with substituents in either the meta or para position of the aniline ring. Horizontal lines represent the mean remaining kinase activity for the grouped data.

(B) Remaining kinase activity of T674I PDGFRα in the presence of 4-anilinoquinazolines containing a para substituent plotted against the molecular weight of the substituent.

(C) Remaining kinase activity of T674I PDGFRα in the presence of 4-anilinoquinazolines with halogen substituents in either the meta or para positions of the aniline ring. Horizontal lines represent the mean remaining kinase activity for the grouped data.

(D) Test compounds used to validate the predictions of the 4-anilinoquinazoline pharmacophore hypothesis.

(E–G) IC_{50} values measured from dose-response curves of the compounds in (D) against T674I PDGFRα in vitro, grouped according to the prediction tested. (E) Substituents at the meta position of the aniline ring are favored over the same substituents at the para position. (F) Large substituents at the para position of the aniline ring decrease potency. (G) Smaller/more electronegative halogen substituents at the meta position of the aniline ring decrease potency toward T674I PDGFRα. Dose response measurements were performed in triplicate. Error bars represent 95% confidence intervals. IC_{50} values are given in Table S3.

inhibitors is the promiscuous nature of these small-molecule compounds. One way to overcome this challenge is to implement a "compound-centric" strategy in which compound libraries are screened broadly against a collection of kinases (Goldstein et al., 2008). Compounds that have undesirable off-target effects are readily identified and eliminated, whereas those with the most promising target spectrum and selectivity are chosen for further analysis and development.

Here, we employed a compound-centric approach to identify inhibitors of disease-associated mutant kinases. We screened a diverse collection of 183 small-molecule kinase inhibitors against 76 mutated kinases derived from 21 cognate wild-type kinases. Initial analysis of the data revealed many unexpected compound/kinase interactions. We found that EGFR/ErbB2/ErbB4 inhibitor targets the highly resistant T790M EGFR mutation with similar potency as afatinib, a structurally related EGFR inhibitor that is FDA-approved. In profiling studies against a panel of 300 wild-type kinases, this compound had notably less off-target activity than afatinib. We also identified opportunities for repurposing FDA-approved kinases for targets other than their intended target. These included several clinical agents that were designed against other targets but also inhibit T674I PDGFRα, a mutation present in imatinib-resistant CEL expressing the FIP1L1-PDGFRα fusion protein. We also identified compounds with activity against ALK, LRRK2, and RET mutant kinases.

In addition to the specific kinase/compound pairs discussed here, we expect that the dissemination of this dataset will lead

to the evaluation of other previously undescribed kinase/compound interactions. The robust quantitative data presented here for mutant kinases, taken together with prior studies focused primarily on wild-type kinases (Anastassiadis et al., 2011; Davis et al., 2011; Fabian et al., 2005; Gao et al., 2013; Karaman et al., 2008), represent a rich resource for compound repurposing and for understanding inhibitor potency and selectivity.

The value of this large dataset rests not only in the identification of potent inhibitors of mutant kinase targets but also in the information provided by compounds with weaker inhibitory activity. Indeed, we illustrated, using T674I PDGFRα, that the aggregate data for 13 4-anilinoquinazoline compounds ranging in potency against this mutant kinase provides predictive structure-activity information to guide subsequent medicinal chemistry efforts. These data are particularly useful in the development of inhibitors for kinases like T674I PDGFRα, for which structural data are lacking. We were able to predict the effects on potency against T674I PDGFRα of chemical modifications to the aniline ring of 6,7-dimethoxy-4-anilinoquinazoline and confirmed these predictions experimentally. Overall, we suggest that large-scale profiling studies using both wild-type and mutant kinases and compound collections of diverse but densely sampled scaffolds will provide the most information-rich approach to compound-centric kinase inhibitor development.

EXPERIMENTAL PROCEDURES

Materials

The majority of kinase inhibitors have been described in a previous study (Anastassiadis et al., 2011). In addition to this set, five additional compounds were profiled: Aurora kinase inhibitor II (CAS no. 331770-21-9, purchased from EMD Biosciences), irfin1 (Anastassiadis et al., 2013; CAS no. 1177970-73-8, purchased from EMD Biosciences), and afatinib (CAS no. 850140-72-6, purchased from LC Laboratories). Olaparib (CAS no. 763113-22-0, purchased from LC Laboratories) and vismodegib (CAS no. 879085-55-9, purchased from LC Laboratories) were included as control compounds. For the dose-response measurements involving 6,7-dimethoxy-4-anilinoquinazoline derivatives, the masses and purities of AG-1478 (CAS no. 153436-53-4, purchased from Selleckchem), CHEMBL94431 (CAS no. 202475-55-6, purchased from Key Organics), EGFR/ErbB2 inhibitor (CAS no. 179248-61-4, purchased from EMD Biosciences), Janex 1 (CAS no. 202475-60-3, purchased from Cayman Chemical), PD153035 (CAS no. 183322-45-4, purchased from Selleckchem), Src kinase inhibitor I (CAS no. 179248-59-0, purchased from EMD Biosciences), and WHI-P180 (CAS no. 211555-08-7, purchased from EMD Biosciences) were confirmed by LC-MS (Waters 2545 binary gradient module, 3100 mass detector, 2487 UV detector set to 254 and 280 nm, and 2424 ELS detector) using a Delta Pak C-18 column (100 Å, 15 μm, 3.9 3 300 mm). Samples were analyzed using a 5%–95% acetonitrile gradient with 0.05% formic acid over 15 min. A description of the kinase constructs and expression systems used for these constructs is given in Table S1.

In vitro Kinase Assays

The Reaction Biology (http://www.reactionbiology.com) HotSpot assay platform was used to measure kinase/inhibitor interactions as described previously (Anastassiadis et al., 2011). In brief, for each reaction, kinase and substrate were mixed in a buffer containing 20 mM HEPES (pH 7.5), 10 mM $MgCl_2$, 1 mM EGTA, 0.02% Brij35, 0.02 mg/mL BSA, 0.1 mM Na_3VO_4, 2 mM DTT, and 1% DMSO. Compounds were then added to each reaction mixture. After a 20-min incubation, ATP (Sigma-Aldrich) and [γ-^{33}P] ATP (PerkinElmer) were added at a final total concentration of 10 μM. Reactions were carried out at room temperature for 2 hr and spotted onto P81 ion exchange cellulose chromatography paper (Whatman). Filter paper was washed in 0.75% phosphoric acid to remove unincorporated ATP. The percent remaining kinase activity relative to a vehicle-containing (DMSO) kinase reaction was calculated for each kinase/inhibitor pair. Outliers were identified and removed as described previously (Anastassiadis et al., 2011). Data were subjected to hierarchical clustering as described previously (Anastassiadis et al., 2011). IC_{50} values were calculated using Prism 5 (GraphPad).

Cell Viability Measurements

Cell viability measurements were carried out using the CellTiter-Glo luminescent cell viability assay (Promega) according to the manufacturer's instructions. Briefly, 10,000 cells were plated in each well of a 96-well plate. Compounds were added to cells, resulting in a DMSO concentration of 0.5% in each well. At 24 hr, CellTiter-Glo reagent was added, and luminescence was measured using an EnSpire multimode plate reader (PerkinElmer). Data were fit to sigmoidal dose-response curves using Prism 5 (GraphPad).

SUPPLEMENTAL INFORMATION

Supplemental Information includes Supplemental Experimental Procedures, four figures, and seven tables and can be found with this article online at http://dx.doi.org/10.1016/j.celrep.2015.12.080.

AUTHOR CONTRIBUTIONS

K.C.D., H.M., and J.R.P. conceived the experiments. K.C.D., S.L., K.Y.H., and Y.W. carried out the experiments. K.D. performed statistical analyses. K.C.D. and J.R.P. wrote the manuscript with input from all authors.

ACKNOWLEDGMENTS

We thank Dr. Jan Cools for providing the Ba/F3-FIP1L1-PDGFRa WT and T674I cell lines and Dr. Cynthia Myers of the FCCC Organic Synthesis Facility for performing the LC-MS analysis. We are grateful to the members of the J.R.P. laboratory for discussions. This work was supported by NIH grants R01 GM083025 (to J.R.P.), T32 CA009035 (to K.C.D.), and P30 CA006927 (to the Fox Chase Cancer Center); the Cancer Kinome Initiative at the Fox Chase Cancer Center; and the Joseph C. Romano Trust Fund. S.L., K.H., Y.W., and H.M. are employees of Reaction Biology.

Received: July 6, 2015
Revised: October 30, 2015
Accepted: December 16, 2015
Published: January 14, 2016

REFERENCES

Anastassiadis, T., Deacon, S.W., Devarajan, K., Ma, H., and Peterson, J.R. (2011). Comprehensive assay of kinase catalytic activity reveals features of kinase inhibitor selectivity. Nat. Biotechnol. *29*, 1039–1045.

Anastassiadis, T., Duong-Ly, K.C., Deacon, S.W., Lafontant, A., Ma, H., Devarajan, K., Dunbrack, R.L., Jr., Wu, J., and Peterson, J.R. (2013). A highly selective dual insulin receptor (IR)/insulin-like growth factor 1 receptor (IGF-1R) inhibitor derived from an extracellular signal-regulated kinase (ERK) inhibitor. J. Biol. Chem. *288*, 28068–28077.

Azam, M., Seeliger, M.A., Gray, N.S., Kuriyan, J., and Daley, G.Q. (2008). Activation of tyrosine kinases by mutation of the gatekeeper threonine. Nat. Struct. Mol. Biol. *15*, 1109–1118.

Balak, M.N., Gong, Y., Riely, G.J., Somwar, R., Li, A.R., Zakowski, M.F., Chiang, A., Yang, G., Ouerfelli, O., Kris, M.G., et al. (2006). Novel D761Y and common secondary T790M mutations in epidermal growth factor receptor-mutant lung adenocarcinomas with acquired resistance to kinase inhibitors. Clin. Cancer Res. *12*, 6494–6501.

Bell, D.W., Gore, I., Okimoto, R.A., Godin-Heymann, N., Sordella, R., Mulloy, R., Sharma, S.V., Brannigan, B.W., Mohapatra, G., Settleman, J., and Haber,

D.A. (2005). Inherited susceptibility to lung cancer may be associated with the T790M drug resistance mutation in EGFR. Nat. Genet. *37*, 1315–1316.

Carey, K.D., Garton, A.J., Romero, M.S., Kahler, J., Thomson, S., Ross, S., Park, F., Haley, J.D., Gibson, N., and Sliwkowski, M.X. (2006). Kinetic analysis of epidermal growth factor receptor somatic mutant proteins shows increased sensitivity to the epidermal growth factor receptor tyrosine kinase inhibitor, erlotinib. Cancer Res. *66*, 8163–8171.

Cools, J., DeAngelo, D.J., Gotlib, J., Stover, E.H., Legare, R.D., Cortes, J., Kutok, J., Clark, J., Galinsky, I., Griffin, J.D., et al. (2003). A tyrosine kinase created by fusion of the PDGFRA and FIP1L1 genes as a therapeutic target of imatinib in idiopathic hypereosinophilic syndrome. N. Engl. J. Med. *348*, 1201–1214.

Davis, M.I., Hunt, J.P., Herrgard, S., Ciceri, P., Wodicka, L.M., Pallares, G., Hocker, M., Treiber, D.K., and Zarrinkar, P.P. (2011). Comprehensive analysis of kinase inhibitor selectivity. Nat. Biotechnol. *29*, 1046–1051.

Eskens, F.A.L.M., Mom, C.H., Planting, A.S.T., Gietema, J.A., Amelsberg, A., Huisman, H., van Doorn, L., Burger, H., Stopfer, P., Verweij, J., and de Vries, E.G. (2008). A phase I dose escalation study of BIBW 2992, an irreversible dual inhibitor of epidermal growth factor receptor 1 (EGFR) and 2 (HER2) tyrosine kinase in a 2-week on, 2-week off schedule in patients with advanced solid tumours. Br. J. Cancer *98*, 80–85.

Fabian, M.A., Biggs, W.H., 3rd, Treiber, D.K., Atteridge, C.E., Azimioara, M.D., Benedetti, M.G., Carter, T.A., Ciceri, P., Edeen, P.T., Floyd, M., et al. (2005). A small molecule-kinase interaction map for clinical kinase inhibitors. Nat. Biotechnol. *23*, 329–336.

Forbes, S.A., Bindal, N., Bamford, S., Cole, C., Kok, C.Y., Beare, D., Jia, M., Shepherd, R., Leung, K., Menzies, A., et al. (2011). COSMIC: mining complete cancer genomes in the Catalogue of Somatic Mutations in Cancer. Nucleic Acids Res. *39*, D945–D950.

Gao, Y., Davies, S.P., Augustin, M., Woodward, A., Patel, U.A., Kovelman, R., and Harvey, K.J. (2013). A broad activity screen in support of a chemogenomic map for kinase signalling research and drug discovery. Biochem. J. *451*, 313–328.

Goldstein, D.M., Gray, N.S., and Zarrinkar, P.P. (2008). High-throughput kinase profiling as a platform for drug discovery. Nat. Rev. Drug Discov. *7*, 391–397.

Gorre, M.E., Mohammed, M., Ellwood, K., Hsu, N., Paquette, R., Rao, P.N., and Sawyers, C.L. (2001). Clinical resistance to STI-571 cancer therapy caused by BCR-ABL gene mutation or amplification. Science *293*, 876–880.

Graczyk, P.P. (2007). Gini coefficient: a new way to express selectivity of kinase inhibitors against a family of kinases. J. Med. Chem. *50*, 5773–5779.

Karaman, M.W., Herrgard, S., Treiber, D.K., Gallant, P., Atteridge, C.E., Campbell, B.T., Chan, K.W., Ciceri, P., Davis, M.I., Edeen, P.T., et al. (2008). A quantitative analysis of kinase inhibitor selectivity. Nat. Biotechnol. *26*, 127–132.

Katakami, N., Atagi, S., Goto, K., Hida, T., Horai, T., Inoue, A., Ichinose, Y., Koboyashi, K., Takeda, K., Kiura, K., et al. (2013). LUX-Lung 4: a phase II trial of afatinib in patients with advanced non-small-cell lung cancer who progressed during prior treatment with erlotinib, gefitinib, or both. J. Clin. Oncol. *31*, 3335–3341.

Klutchko, S.R., Zhou, H., Winters, R.T., Tran, T.P., Bridges, A.J., Althaus, I.W., Amato, D.M., Elliott, W.L., Ellis, P.A., Meade, M.A., et al. (2006). Tyrosine kinase inhibitors. 19. 6-Alkynamides of 4-anilinoquinazolines and 4-anilinopyrido[3,4-d]pyrimidines as irreversible inhibitors of the erbB family of tyrosine kinase receptors. J. Med. Chem. *49*, 1475–1485.

Kosaka, T., Yatabe, Y., Endoh, H., Yoshida, K., Hida, T., Tsuboi, M., Tada, H., Kuwano, H., and Mitsudomi, T. (2006). Analysis of epidermal growth factor receptor gene mutation in patients with non-small cell lung cancer and acquired resistance to gefitinib. Clin. Cancer Res. *12*, 5764–5769.

Ladanyi, M., and Pao, W. (2008). Lung adenocarcinoma: guiding EGFR-targeted therapy and beyond. Mod. Pathol. *21* (*Suppl 2*), S16–S22.

Li, D., Ambrogio, L., Shimamura, T., Kubo, S., Takahashi, M., Chirieac, L.R., Padera, R.F., Shapiro, G.I., Baum, A., Himmelsbach, F., et al. (2008). BIBW2992, an irreversible EGFR/HER2 inhibitor highly effective in preclinical lung cancer models. Oncogene *27*, 4702–4711.

Lierman, E., Folens, C., Stover, E.H., Mentens, N., Van Miegroet, H., Scheers, W., Boogaerts, M., Vandenberghe, P., Marynen, P., and Cools, J. (2006). Sorafenib is a potent inhibitor of FIP1L1-PDGFRalpha and the imatinib-resistant FIP1L1-PDGFRalpha T674I mutant. Blood *108*, 1374–1376.

Lierman, E., Michaux, L., Beullens, E., Pierre, P., Marynen, P., Cools, J., and Vandenberghe, P. (2009). FIP1L1-PDGFRalpha D842V, a novel panresistant mutant, emerging after treatment of FIP1L1-PDGFRalpha T674I eosinophilic leukemia with single agent sorafenib. Leukemia *23*, 845–851.

Metzgeroth, G., Erben, P., Martin, H., Mousset, S., Teichmann, M., Walz, C., Klippstein, T., Hochhaus, A., Cross, N.C.P., Hofmann, W.-K., and Reiter, A. (2012). Limited clinical activity of nilotinib and sorafenib in FIP1L1-PDGFRA positive chronic eosinophilic leukemia with imatinib-resistant T674I mutation. Leukemia *26*, 162–164.

Paez, J.G., Jänne, P.A., Lee, J.C., Tracy, S., Greulich, H., Gabriel, S., Herman, P., Kaye, F.J., Lindeman, N., Boggon, T.J., et al. (2004). EGFR mutations in lung cancer: correlation with clinical response to gefitinib therapy. Science *304*, 1497–1500.

Pao, W., Miller, V.A., Politi, K.A., Riely, G.J., Somwar, R., Zakowski, M.F., Kris, M.G., and Varmus, H. (2005). Acquired resistance of lung adenocarcinomas to gefitinib or erlotinib is associated with a second mutation in the EGFR kinase domain. PLoS Med. *2*, e73.

Pines, G., Köstler, W.J., and Yarden, Y. (2010). Oncogenic mutant forms of EGFR: lessons in signal transduction and targets for cancer therapy. FEBS Lett. *584*, 2699–2706.

Sadovnik, I., Lierman, E., Peter, B., Herrmann, H., Suppan, V., Stefanzl, G., Haas, O., Lion, T., Pickl, W., Cools, J., et al. (2014). Identification of Ponatinib as a potent inhibitor of growth, migration, and activation of neoplastic eosinophils carrying FIP1L1-PDGFRA. Exp. Hematol. *42*, 282–293.e4.

Uitdehaag, J.C.M., de Roos, J.A.D.M., van Doornmalen, A.M., Prinsen, M.B.W., de Man, J., Tanizawa, Y., Kawase, Y., Yoshino, K., Buijsman, R.C., and Zaman, G.J.R. (2014). Comparison of the cancer gene targeting and biochemical selectivities of all targeted kinase inhibitors approved for clinical use. PLoS ONE *9*, e92146.

von Bubnoff, N., Gorantla, S.P., Thöne, S., Peschel, C., and Duyster, J. (2006). The FIP1L1-PDGFRA T674I mutation can be inhibited by the tyrosine kinase inhibitor AMN107 (nilotinib). Blood *107*, 4970–4971, author reply 4972.

Yun, C.-H., Mengwasser, K.E., Toms, A.V., Woo, M.S., Greulich, H., Wong, K.-K., Meyerson, M., and Eck, M.J. (2008). The T790M mutation in EGFR kinase causes drug resistance by increasing the affinity for ATP. Proc. Natl. Acad. Sci. USA *105*, 2070–2075.

Zhang, J., Yang, P.L., and Gray, N.S. (2009). Targeting cancer with small molecule kinase inhibitors. Nat. Rev. Cancer *9*, 28–39.